2

OFFICE OF NAVAL RESEARCH

Grant N00014-90-J-1235

R & T Code 4133020

Technical Report No. 21

Application of the A.C. Admittance Technique to Double Layer Studies on Polycrystalline Gold Electrodes

by

W. Ronald Fawcett, Zuzana Kováčová, Artur J. Motheo and Colby A. Foss, Jr.

Prepared for Publication

in

Journal of Electroanalytical Chemistry

Department of Chemistry
University of California
Davis, CA 95616

February 24, 1992

Reproduction in whole or in part is permitted
for any purpose of the United States Government

"This document has been approved for public release
and sale; its distribution is unlimited"

REPORT DOCUMENTATION PAGE

Form Approved
OMB No. 0704-0188

1. AGENCY USE ONLY (Leave blank)	2. REPORT DATE	3. REPORT TYPE AND DATES COVERED
	Febr. 24, 1992	Technical

4. TITLE AND SUBTITLE

Application of the A.C. Admittance Technique to Double Layer Studies on Polycrystalline Gold Electrodes

5. FUNDING NUMBERS

N00014-90-J-1235

6. AUTHOR(S)

W. Ronald FAwcett, Zuzana Kovačová, Artur J. Motheo, and Colby A. Foss, Jr.

7. PERFORMING ORGANIZATION NAME(S) AND ADDRESS(ES)

Department of Chemistry
University of California
Davis, CA 95616

8. PERFORMING ORGANIZATION REPORT NUMBER

No. 21

9. SPONSORING/MONITORING AGENCY NAME(S) AND ADDRESS(ES)

Office of Naval Research
800 N. Quincy
Arlington, VA 22217-5000

10. SPONSORING/MONITORING AGENCY REPORT NUMBER

11. SUPPLEMENTARY NOTES

Prepared for publication in Journal of Electroanalytical Chemistry

12a. DISTRIBUTION/AVAILABILITY STATEMENT

Unclassified

12b. DISTRIBUTION CODE

13. ABSTRACT (Maximum 200 words)

A detailed examination of the dependence of the a.c. admittance of a cell containing a polycrystalline gold electrode has been made in the double layer region as a function of d.c. potential, a.c. frequency and electrode history. It is shown that the interfacial impedance of a gold electrode with a carefully prepared surface can be treated under these circumstances as a constant phase element when it is in contact with an aqueous solution containing 0.05 M $KClO_4$. Analysis of the frequency dependence of the cell impedance gives the surface inhomogeneity parameter n which turns out to be very close to unity. Although the electrode surface is only slightly inhomogeneous on a microscopic scale, a very large frequency dispersion of the impedance is observed experimentally. A method of estimating the true specific capacity of the electrode is presented, and conditions for carrying out the experiments in a reproducible manner discussed.

14. SUBJECT TERMS

double layer at gold/solution interface, a.c. admittance techniques, constant phase element model

15. NUMBER OF PAGES

16. PRICE CODE

17. SECURITY CLASSIFICATION OF REPORT	18. SECURITY CLASSIFICATION OF THIS PAGE	19. SECURITY CLASSIFICATION OF ABSTRACT	20. LIMITATION OF ABSTRA
unclassified	unclassified	unclassified	unclassified

Application of the A.C. Admittance Technique to Double Layer Studies on Polycrystalline Gold Electrodes

W. Ronald Fawcett*, Zuzana Kováčová, Artur J. Motheo[‡] and Colby A. Foss Jr.

Department of Chemistry
University of California
Davis, CA 95616
U.S.A.

[‡] On leave from the Instituto de Fisica e Quimica de Sao Carlos, USP, Sao Carlos, SP 13560, Brazil

Summary

A detailed examination of the dependence of the a.c. admittance of a cell containing a polycrystalline gold electrode has been made in the double layer region as a function of d.c. potential, a.c. frequency and electrode history. It is shown that the interfacial impedance of a gold electrode with a carefully prepared surface can be treated under these circumstances as a constant phase element when it is in contact with an aqueous solution containing 0.05 M $KClO_4$. Analysis of the frequency dependence of the cell impedance gives the surface inhomogeneity parameter n which turns out to be very close to unity. Although the electrode surface is only slightly inhomogeneous on a microscopic scale, a very large frequency dispersion of the impedance is observed experimentally. A method of estimating the true specific capacity of the electrode is presented, and conditions for carrying out the experiments in a reproducible manner discussed.

Experimental

Instrumentation

The admittance data were obtained using an experimental set-up designed for dropping mercury electrodes but adapted here to work at solid electrodes with a fixed delay time after application of the d.c. potential to the electrode. A block diagram of the system with which both a.c. admittance and cyclic voltammetric data were obtained is shown in Fig. 1. The electrode potentiostatic control was provided by a PAR 174A Polarographic Analyzer, and the timer/trigger function was provided by a PAR 303A Static Mercury Drop Apparatus. In the case of cyclic voltammetry measurements, the linear voltage ramp was obtained from a PAR 175 Universal Programmer, and the output current and voltage were recorded on an X-Y recorder. A cyclic voltammogram was always recorded first on the electrode to ascertain that the electrode surface had been properly prepared and that the level of impurities in the solution was sufficiently low. In the case of a.c. admittance measurements both the linear potential ramp and the a.c. signal were provided by a Solartron 1250 Frequency Response Analyzer, and fed into the external input of the PAR 174A through an attentuator. The attentuator was introduced in order to avoid signal noise from the a.c. signal generator which is present at low amplitudes. The a.c. signal level applied to the cell was 10 mV peak-to-peak. In the admittance experiment, the potential was stepped in 25 mV increments in a pre-programmed direction. The potential change was triggered by the PAR 303A system which allowed a new potential to be applied to the electrode for a known number of seconds before the admittance was measured. In this way, the effect of the delay time on the admittance data was examined.

Most of the collection parameters were controlled through a serial interface (RS 323) between the Solartron 1250 and an IBM PC-XT clone. Drop time, current gain and initial d.c. potential were set manually on the PAR 174A. As part of the data analysis to isolate the cell impedance, the phase shifts inherent in the potentiostat and the cables were determined. This was done by collecting admittance data for a "dummy" cell which was a simple standard resistor and capacitor in series with an impedance comparable to that of the actual cell. This procedure provided a correction factor which was applied to the raw admittance data to determine the actual admittance of the electrochemical cell.

The Gold Electrode

The working electrode was a polycrystalline gold rod (99.995 % pure) prepared by fusion in a graphite mold (diameter = 2.54 mm) at 1200 °C under vacuum. Electrical contact was made via a gold wire fused at one of the ends of the rod. The electrode surface was prepared according to well established procedures.[1,5,6] Firstly, the rod was washed with aqua regia to remove the top layer of gold with collected impurities. After this, the edges of the crystallographic planes are observable with the naked eye, confirming the material's polycrystalline nature. In the second step, the electrode was electropolished, following the procedure outlined by Peck and Nakahara[10], in order to provide surface conditions for which solution creep is avoided in the meniscus configuration.[1] This was followed by mechanical polishing of the free end of the gold cylinder with successively finer grades of Alumina powder down to 0.05 µm. Then the electrode was annealed at 700 °C under vacuum, and chemically treated in a series of solutions involving HF, NaOH, HNO_3 and H_2SO_4 in that order as described previously.[11] Finally, the electrode was kept immersed in high quality water until it was about to be used in the electrochemical experiment. At that point it was flame annealed in a natural gas/air flame and then quenched in nanopure water before being transferred to the cell. The geometric area of the cylinder end in contact with the solution was ~0.05 cm^2; the exact area was determined using dial calipers to measure the diameter of the Au rod after completion of the electrochemical experiments.

The Cell and Other Electrodes

The cell was of conventional design and incorporated the gold working electrode, a gold counter electrode and a commercial saturated calomel electrode (SCE). The gold electrode was mounted in a glass tube between two teflon holders which allowed the vertical position of the electrode to be continuously varied. The electrode system was clamped to the body of the cell via a ball joint which allowed variation in the angle with which the end of the gold cylinder comes into contact with the solution. The counter electrode was a gold wire spiral of relatively large area. It was submitted to the same chemical treatment as the working electrode and flame annealed before being placed in the cell. The SCE was connected to the main body of the cell through a Luggin capillary.

Electrolyte and Solvent Purification

All water used in the experiments was of high quality. It was prepared in a Barnstead water purification system, and had a resistivity in the range 17.8 to 18.3 MΩ cm. This water was used in the cleaning procedures for the cell, in the flame annealing step, in salt purification, as well as in preparing the electrolyte solutions. The electrolyte used was $KClO_4$ (Fluka); it was calcined under vacuum at 600 °C, twice recrystallized from high quality water, and then calcined again.

Results

Cyclic Voltammetry

As demonstrated in previous work[1,5,611], cyclic voltammetry is a valuable tool for testing the purity of the solution and the state of cleanliness of the electrode surface. Hence, each admittance experiment was preceded by a cyclic voltammetric measurement. A typical result obtained in the present work is shown in Fig. 2. The features agree completely with those reported recently in the literature.[5,6,11] The symmetry of the current-voltage curve with respect to $i = 0$ in the double layer region demonstrates that the solution is oxygen free, and that no solution creep up the electrode wall is occurring. One may note a slight increase in the slope of the current-voltage curve on the negative sweep near -0.8 V which indicates the onset of hydrogen deposition. This feature was used as an experimental indication of the negative limit for double layer measurements on gold. The positive limit was set at 0.625 V, well negative of the region in which noticeable oxidation of the gold surface begins.

A.C. Admittance Measurements

A.C. admittance data were gathered as a function of d.c. potential and frequency. In general, the gold electrode was flame annealed before each polarization and a series of slow oxidation-reduction cycles applied to strip off the layers affected by annealing. In- and out-of-phase admittance data were obtained at six frequencies in the range 25 to 250 Hz beginning at a d.c. potential of -0.85 V against a S.C.E. in 0.05 M $KClO_4$. These data were then converted to the equivalent resistance and capacitance assuming the simple series circuit used to analyze admittance data for the mercury/solution interface. Thus, the resistance is given by

$$R = \frac{A_R}{A^2 + A^2} \tag{1}$$

and the capacitance by

$$C = \frac{A_R + A_I}{\omega A_I} \tag{2}$$

where A_R is the in-phase (real) component of the admittance, A_I, its out-of-phase (imaginary) value, and ω, the angular velocity associated with the a.c. signal. It is clear from the resulting data (Figs. 3 and 4) that there is considerable frequency dispersion and that the extent of dispersion increases as the electrode potential becomes more positive. Reproducibility of individual data sets at a fixed frequency was better than 1%. As will be seen below, the same low level of error is found for the derived solution resistance R_s and double layer capacitance, C.

The general features of the capacity curves observed here are qualitatively similar to those reported earlier by Clavilier and Huong.[3] Thus, one finds a high capacity maximum in the vicinity of -0.3 V and a lower one at +0.25 V. The central minimum on the capacity curves which is attributed to the low value of the diffuse layer capacity at the potential of zero charge[3] occurs at 0.048 V. This result is in excellent agreement with that reported earlier by Clavilier and Van Huong.

When the electrode is polarized from positive to negative potentials, the shape of the capacity curve is qualitatively different at positive potentials. This result is taken as evidence for the presence of a small amount of oxide on the electrode which is presumably reduced when the electrode potential is more negative than 0.0 V. The changes in R with potential are attributed in large part to the fact that the equivalent circuit representation used to obtain the results presented is naive, a correct representation being somewhat more detailed.[4,7]

As mentioned above, each admittance measurement was made after a fixed delay time which varied from 1 to 9 s. The purpose of this feature of the experimental method was to demonstrate that the system had indeed come to equilibrium and that the interfacial admittance does not depend on time due to slow adsorption of organic impurities from the bulk. In the present case, no significant variation in admittance was found as a function of delay time. This result is taken as further evidence that the electrolyte solutions prepared for these experiments were of high quality, that is, relatively free of organic contaminants. For all experimental data presented here, the delay time was 1 s.

Analysis of the Frequency Dependence of the Impedance

As one would expect, the capacity of the electrode/solution interface estimated use the simple R, C series representation varied with frequency of the applied a.c. voltage. Thus, the capacity data presented above are naive and significantly in error with respect to the true specific capacity of the interface. It is generally recognized[4,7] that the impedance of a system with a rough electrode immersed in an electrolyte solution may be written

$$Z = R_S + \frac{R_S^{1-n}}{(j\omega C)^n} \tag{3}$$

where R_S is the solution resistance, C, the capacitance of the interface, ω, the angular frequency, and n, a dimensionless number between 0.5 and 1.0 related to surface roughness. Expanding the second term into its real and imaginary parts, one obtains[4]

$$Z = R_S + \frac{R_S^{1-n}}{(\omega C)^n} \{\sin[(1-n)\pi/2] - j\cos[(1-n)\pi/2]\} \tag{4}$$

This equation shows that the resistance and capacity affect both the in- and out-of-phase components of the impedance and explains a major part of the fluctuation in the "naive" resistance and capacity with potential found when the data are analyzed on the basis of a simple R, C series circuit (see Figs. 3 and 4). However, since the exponent n is close to one, as will be shown below, the sine term in the above expression is very small and the cosine term close to unity. Otherwise stated, the angle (1-n) π/2 which defines the degree of departure of the constant phase element, $R_S^{1-n}/(\omega C)^n$, from the vertical in an impedance plot is very small. As a result, any experimental error will have a large effect on the sine term but a relatively small effect on the cosine term.

The method of analysis adopted here was to determine first the exponent, n, by examining the frequency dependence of the out-of-phase component of the impedance, Z_{out}, which was calculated from the experimental admittance using the usual transformation. According to eq. (2), the dependence of Z_{out} on the angular frequency ω is given by

$$\ln Z_{out} = \ln \cos[(1-n)\pi/2] - n \ln C - n \ln \omega + (1-n) \ln R_s \quad (5)$$

It follows that a plot of ln Z_{out} against ln ω should be linear with a slope equal to -n. Representative plots at varying potentials for data obtained at six frequencies in the range 25 to 250 Hz are shown in Fig.5. It is apparent that there is an excellent linear relationship between ln Z_{out} and ln ω, the slope being in the range from 0.94 to 1.00. The solution resistance was determined by plotting Z_{in} against Z_{out}, typical plots being shown in Fig. 6. The value of R_s obtained from the limiting value of Z_{in} as the frequency goes to infinity ($Z_{out} \rightarrow 0$) was close to 450 Ω at negative potentials, but some variation with electrode potential was found. Ideally, one should be able to determine the exponent, n, from the slopes of the plots shown in Fig. 6 (see eq. 4). However, this is not considered to be a reliable method of determining this parameter, since small errors in the phase angle measurement lead to large errors in Z_{in} but relatively small errors in Z_{out}. On the other hand, one does not anticipate significant error in the value of R_s obtained from the intercept of the plot shown in Fig. 6 due to possible errors in the phase angle determination. Finally, the specific capacitance was determined at each potential from the out-of-phase impedance Z_{out} using eq. (3). Values of the specific capacity calculated using eq. (3) and the data obtained here are shown in Fig. 7. These results show that the estimated capacity of the basis of CPE model is very close to that observed at 25 Hz.

Values of the parameter, n estimated at each value of the d.c. potential where data were obtained are shown as a function of potential in Fig. 8. The limiting value of n at negative potentials is 0.998 on the basis of the smooth curve drawn through these data. This result shows that the gold electrode behaves almost as if it were perfectly smooth under the conditions that the experiment is initiated. As the d.c. potential is made more positive, surface inhomogeneity becomes more important, and n, decreases reaching values below 0.95 at the most positive potentials. This corresponds to a CPE having the out-of-phase component very close to 90° with respect to the in-phase value changing such that the out-of-phase component makes an angle of approximately 85° to the in-phase component. It is interesting to speculate on the reasons for this change. One may be that the chemisorption of water, a process which occurs as the electrode is polarized in the positive direction, is preferred on certain faces of the polycrystalline surface with respect to others. In the most positive region where surface oxidation begins the parameter, n, drops rapidly indicating that surface inhomogeneity is much more important as one would expect. A second reason for the change in n with potential is that the gold surface is expected to undergo reconstruction. Reconstruction phenomena have been examined in some detail by Kolb and coworkers[10,11] for single crystal gold electrodes.

The change in the parameter, n, is accompanied by a change in the net solution resistance as shown by the data presented in Fig. 9. At the most negative potentials, this has a value close to 450 Ω but steadily increases to ~470 Ω at a potential of 0.4 V. Some decrease in total resistance is seen at more positive potentials. This is undoubtedly related to the onset of oxidation and the presence of a small faradaic component in the total admittance observed experimentally.

The scatter in the results for both the resistance R_s and the parameter, n demonstrate that these quantities are not determined as precisely as the interfacial capacity C. In the case of R_s, the scatter is chiefly due to error in the value of the in-phase component of the impedance Z_R. Since the value of 1-n is close to zero, small changes in n can result in relatively larger changes in Z_R. Thus, the extrapolation procedure used to estimate R_s (see Fig. 6) is subject to more error than the procedures used to estimate the other parameters. However, it should be noted that errors in R_s do not lead to large errors in the estimation of the capacity C. This follows from the fact that the contribution of R_s to the CPE is small, being raised to the power (1-n), the resulting contribution to the error being correspondingly smaller. Thus, if the largest value of R_s is 470 Ω and the corresponding value of n, 0.96, the contribution $R^{(1-n)}$ to the CPE is 1.28. At the same time, if the random error in R amounts to 2%, the corresponding random error in $R^{(1-n)}$ is 0.1%. The scatter in the value of n with respect to a smooth curve fitted to the data amounts on the average to ±2 parts per thousand. This is attributed to instrumental noise and failure of the CPE model to describe the system exactly as the inhomogeneity of the interface changes due to change in electrode potential. However, when one considers all of the results presented here, it is clear that the CPE model certainly gives good description of the system. Not only can it be used to derive values of the interfacial capacity but it can also provide a qualitative picture of changes in surface homogeneity with potential.

Discussion

The above analysis demonstrates that the frequency dispersion observed in the admittance of a polycrystalline gold electrode in an aqueous electrode solution can be understood on the basis of an equivalent circuit model in which the interface is represented as a constant phase element.[4,7] In addition, values of the specific capacity calculated using these data are quite reasonable in terms of estimates made previously.[1,5,6,12] On the basis of the value of the inhomogeneity parameter, n, it is concluded that gold surfaces prepared by the methods outlined by Hamelin[1] are very smooth since, n, is quite close to one. In spite of this fact, a large variation in experimental admittance with frequency is found at positive potentials within the polarizable range on gold so that one may not use admittance data obtained at a single frequency to obtain a quantitative estimate of the specific interfacial capacity unless one has independent knowledge of the parameter, n. The present results also provide evidence that the parameter, n, changes with potential, and that this change may be connected with the processes which lead up to oxidation of the surface. This particular feature of the admittance data is not available when interfacial capacity is determined using the chronocoulometric technique[5,6,12] and provides additional valuable information regarding the state of the interface. For instance, it would be interesting to examine both the variation in interfacial capacity and the inhomogeneity parameter with electrode potential for different single crystal faces of the gold electrode. Although studies of the variation in interfacial capacity with crystallographic orientation have been made, no information is available on the corresponding variation in the effects of interfacial inhomogeneity. The fact that one should expect the effects of inhomogeneity at a metal surface which is not atomically smooth has been demonstrated by Van den Eeden et al. using quantum mechanical methods.[13] They showed that the capacity distribution results from coordinate-dependent charge redistribution caused by a change of electric field strength at the electrode surface. This distribution leads to a deviation from purely capacitive behaviour of the solid metal/electrolyte interface but does not explain the CPE behaviour.[13]

It is interesting to compare the present analysis based on the CPE with an analysis using the method of fractals.[9] Fractal models for rough electrodes have been discussed in detail in the recent literature[9] and applied to the problem of diffusion to rough interfaces[14] and the impedance of polarizable rough electrodes.[15] The expression derived for the interfacial impedance for a rough electrode with fractal geometry has the same form as that given here for the CPE (eq. 3). On the basis of a recent analysis[9], it is clear that the fractal analysis is not appropriate for the present system. Pakossy[9] has also pointed out that there is no unique relationship between the inhomogeneity parameter, n, discussed here and the fractal dimension. The present results show clearly that the gold interface departs so little in its properties from those of a perfectly homogeneous interface, that the CPE model can describe its behaviour very well.

Acknowledgements

The authors are indebted to Dr. A. Hamelin and Professor J. Lipkowski for their careful and patient explanation of the procedures used to obtain reproducible gold electrode surfaces. Helpful comments regarding the CPE model were made by Professor A. Lasia. This work was supported by a grant from the Office of Naval Research, Washington. A.J.M. thanks the Conselho de Desenvolvimento Cientifico e Tecnologico, Brazil for a fellowship held during his stay in this laboratory.

References

1. Hamelin, A. Modern Aspects Electrochem. 1985, 16, 1.
2. Vorotyntsev, M.A. Modern Aspects Electrochem. 1986, 17, 131.
3. Clavilier, J.; Van Huong, C.N. J. Electroanal.Chem. 1977, 80, 101.
4. Scheider, W. J. Phys. Chem. 1975, 79, 127.
5. Richer, J.; Lipkowski, J. J. Electrochem. Soc. 1986, 133, 121.
6. Iannelli, A.; Richer, J.; Lipkowski, J. Langmuir, 1989, 5, 466.
7. Brug, G.J.; Van den Eeden, A.L.G.; Sluyters-Rehbach, M.; Sluyters, J.H. J. Electroanal. Chem. 1984, 176, 275.
8. Macdonald, J.R., editor, Impedance Spectroscopy, Wiley, New York, 1987.
9. Pajkossy, T. J. Electroanal. Chem. 1991, 300, 1.
10. Kolb, D.M.; Schneider, J. Electrochim. Acta, 1986, 31, 929.
11. Zei, M.S.; Lehmpfuhl, G.; Kolb, D.M. Surface Science, 1989, 221, 23.
12. Richer, J.; Lipkowski, J. J. Electroanal. Chem. 1988, 251, 217.
13. Van den Eeden, A.L.G.; Sluyters, J.H.; van Lenthe, J.H. J. Electroanal. Chem. 1984, 171, 195.
14. Nyikos, L.; Pajkossy, T. Electrochim. Acta, 1986, 31, 1347.
15. Nyikos, L.; Pajkossy, T. Electrochim. Acta, 1985, 30, 1535.

Legends for Figures

Figure 1. Schematic diagram of the experimental system used to acquire a.c. admittance data and cyclic voltammetric curves.

Figure 2. Typical cyclic voltammogram obtained at the polycrystalline Au/aqueous solution interface.

Figures 3. Resistance of the electrochemical cell with a polarizable Au electrode in 0.05 M $KClO_4$ estimated from a.c. admittance data as a function of d.c. potential using eq. (1). Data were obtained in six frequencies: (•) 25, (▲) 40, (◆) 63, (▼) 100, (■) 160 and (o) 250 Hz.

Figure 4. Capacitance of the electrode/solution interface for a polarizable Au electrode in 0.05 M $KClO_4$ estimated from a.c. admittance data as a function of d.c. potential using eq. 92). Data were obtained at six frequencies: (•) 25, (▲) 40, (◆) 63, (▼) 100, (■) 160 and (o) 250 Hz.

Figure 5. Plots of the out-of-phase impedance Z_i against the frequency of the a.c. signal on logarithmic scales for data obtained at fixed d.c. potentials as indicated.

Figure 6. Plots of the the in-phase impedance Z_R against the out-of-phase impedance Z_i for data obtained at varying frequencies and constant d.c. potential as indicated.

Figure 7. Capacity of the polycrystalline gold electrode in 0.05 M $KClO_4$ as a function of electrode potential.

Figure 8. Inhomogeneity parameter, n, for the polycrystalline gold electrode in 0.05 M $KClO_4$ as a function of electrode potential on the basis of data for the cell admittance as a function of frequency.

Figure 9. Solution resistance R_S as a function of electrode potential on the basis of data for the cell admittance as a function of frequency.

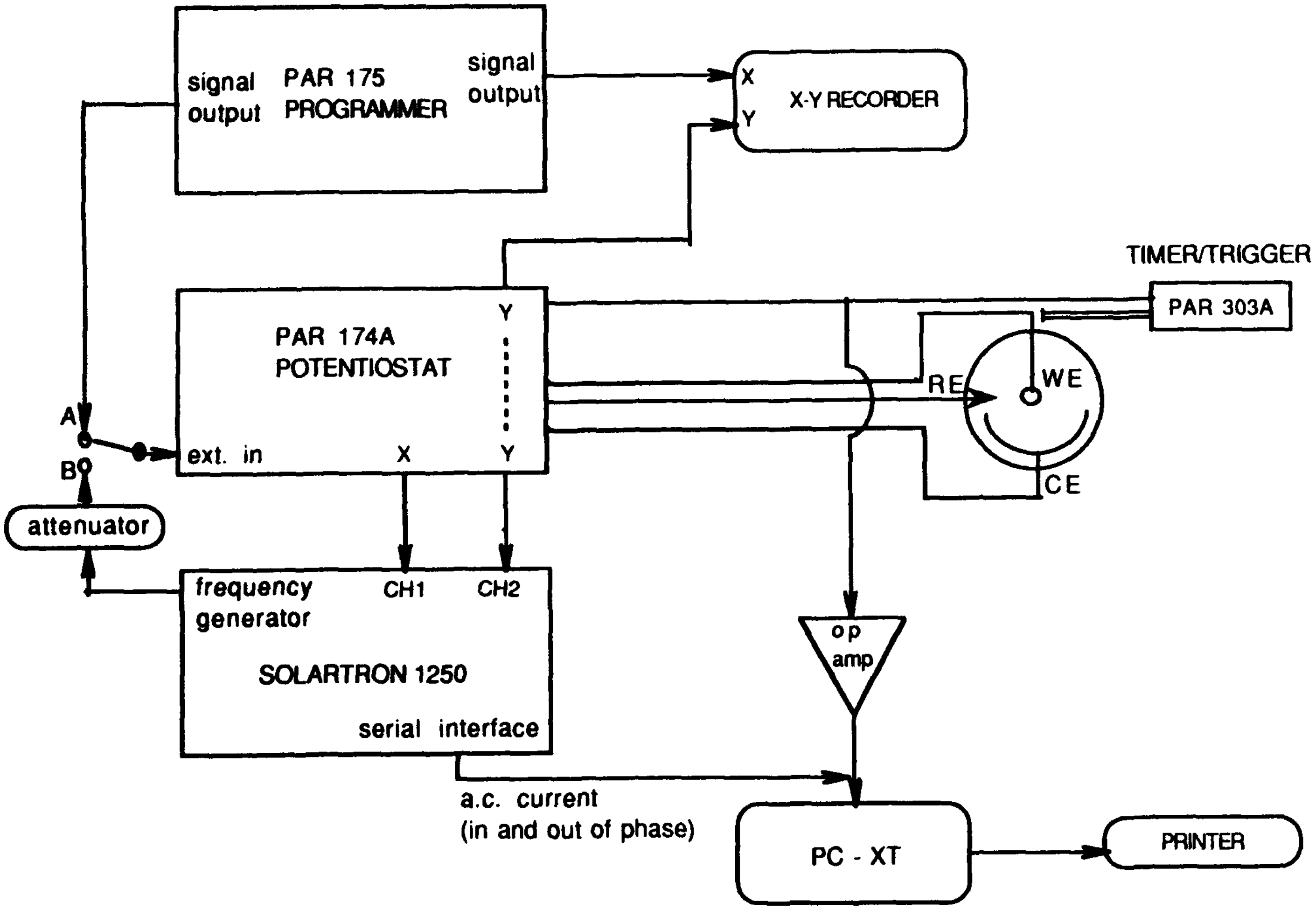
signal
output
PAR 175
PROGRAMMER
signal
output
X
Y
X-Y RECORDER
TIMER/TRIGGER
PAR 303A
A
B
attenuator
PAR 174A
POTENTIOSTAT
Y
ext. in
X
Y
RE
WE
CE
frequency
generator
CH1
CH2
SOLARTRON 1250
serial interface
op
amp
a.c. current
(in and out of phase)
PC - XT
PRINTER

Fig. 1

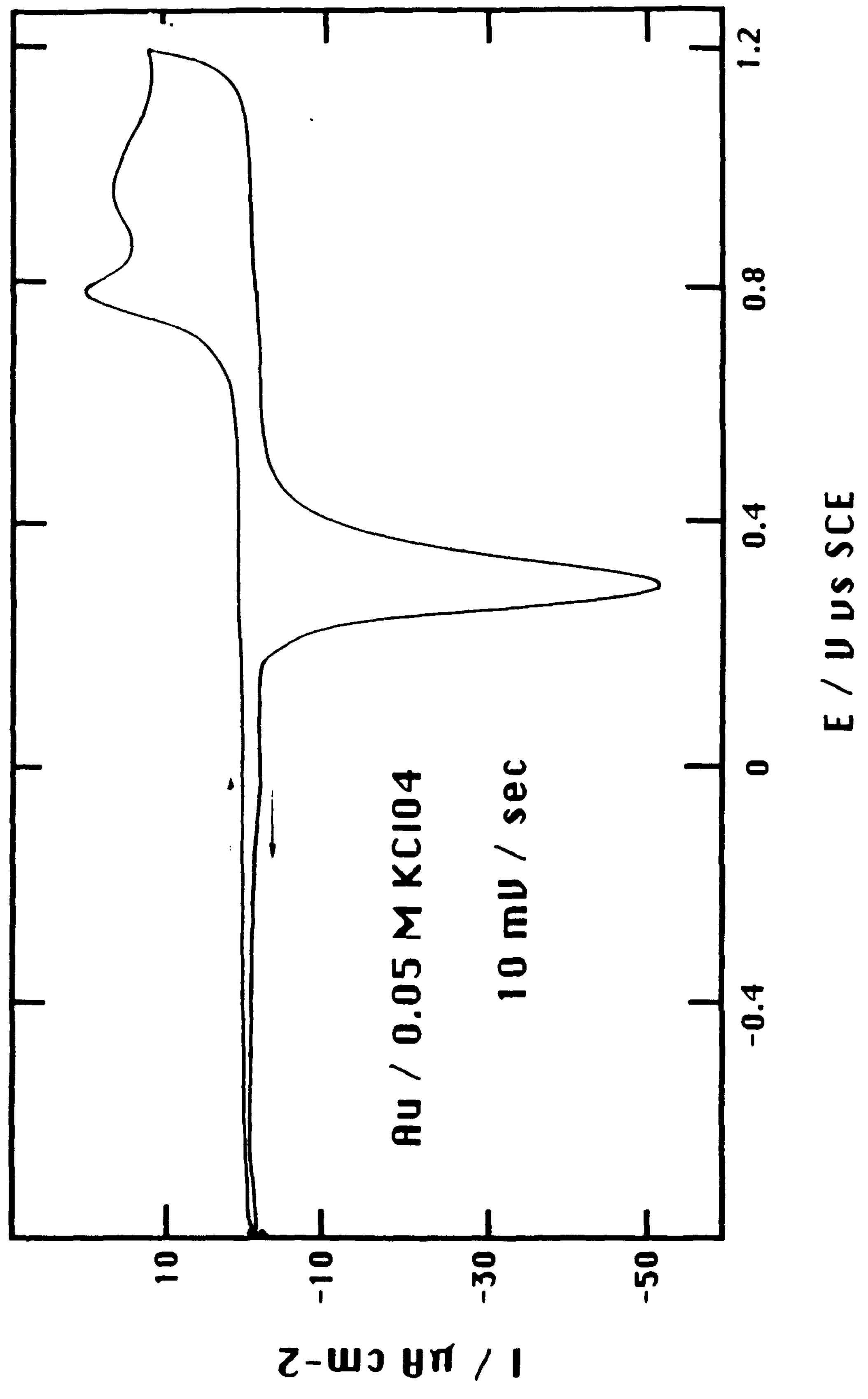

Fig2

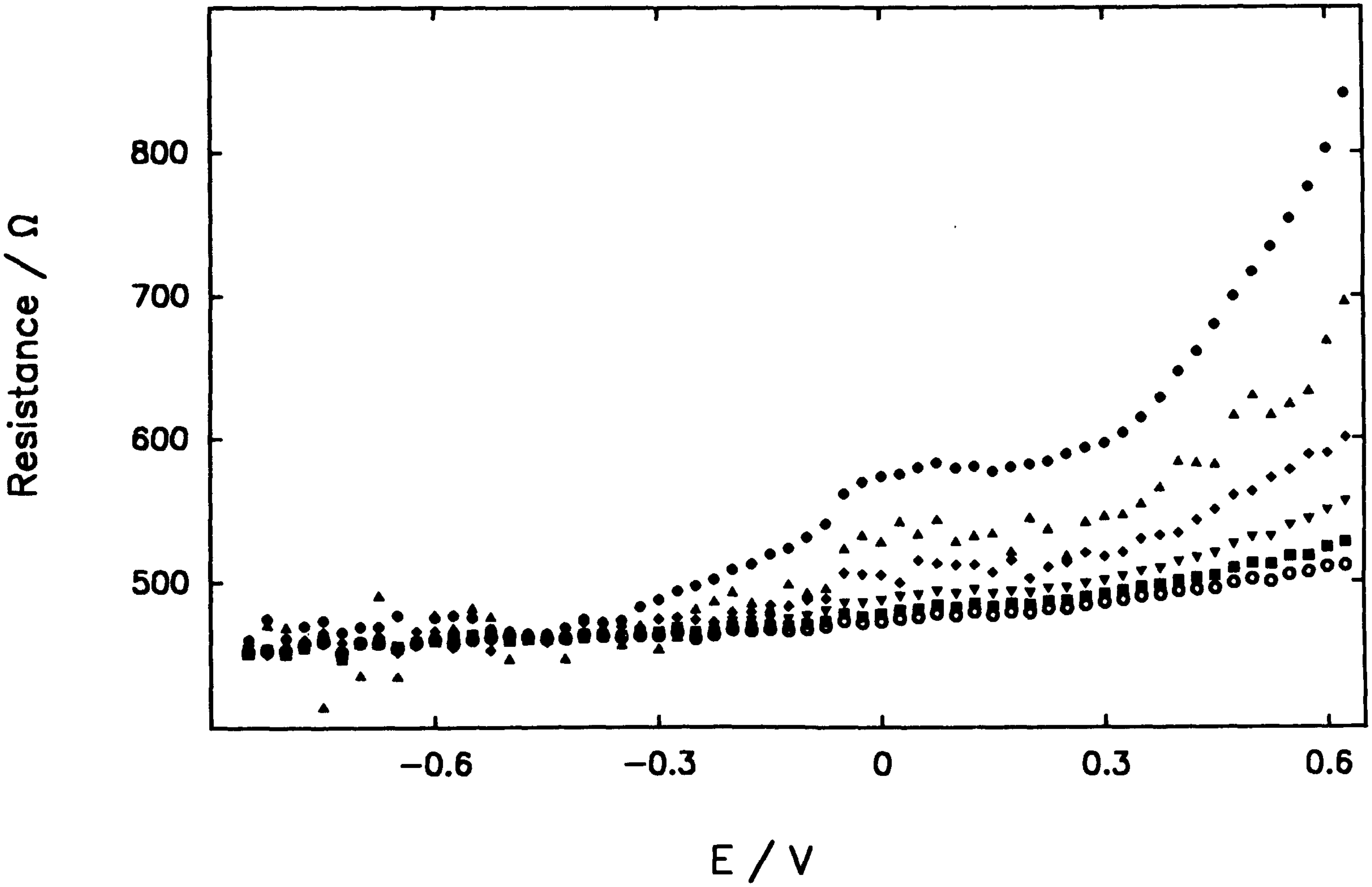

Fig 3

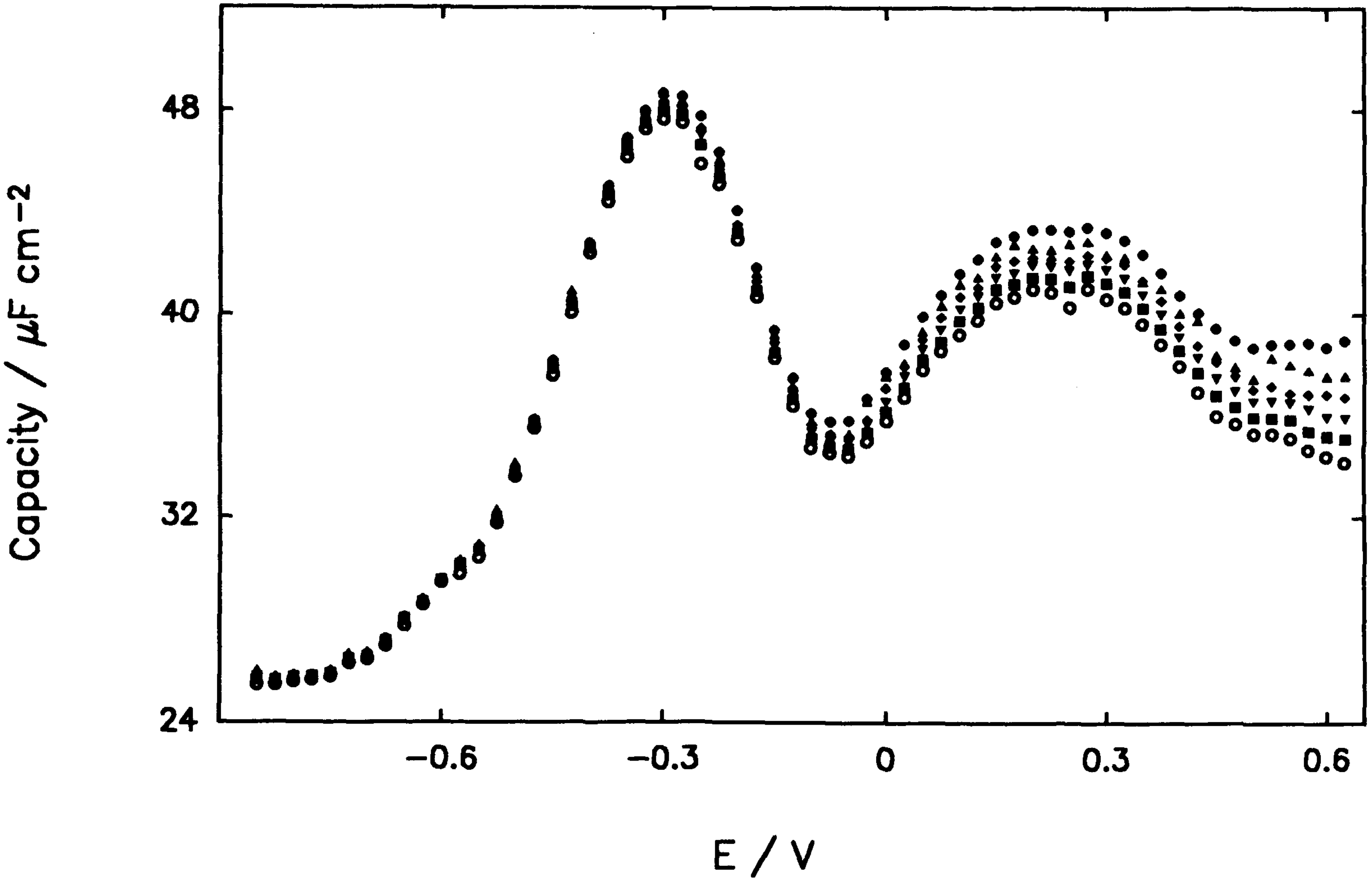

Fig 4

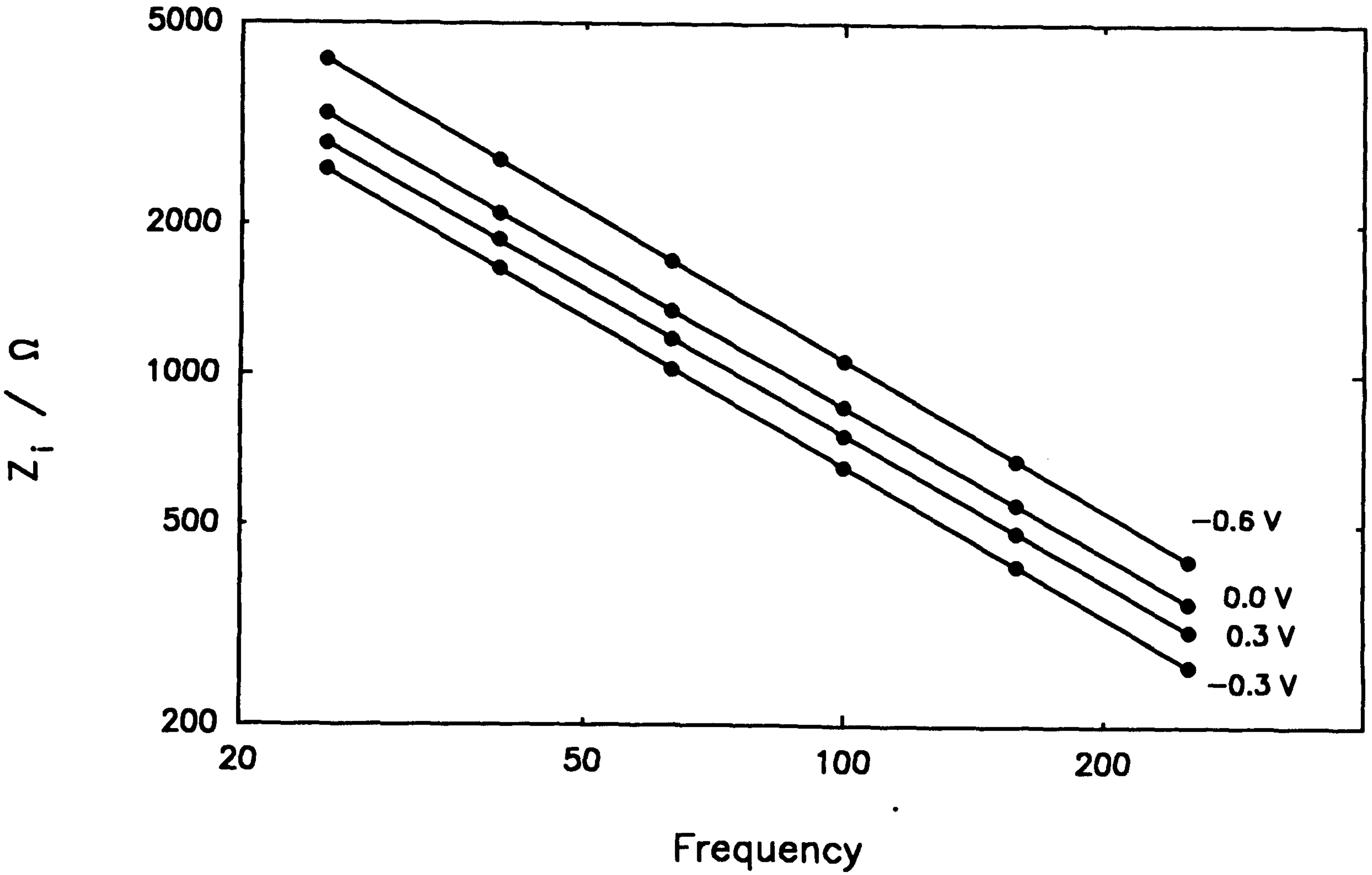
5000
2000
1000
500
200
Z_i / Ω
20
50
100
200
Frequency
−0.6 V
0.0 V
0.3 V
−0.3 V

Fig 5

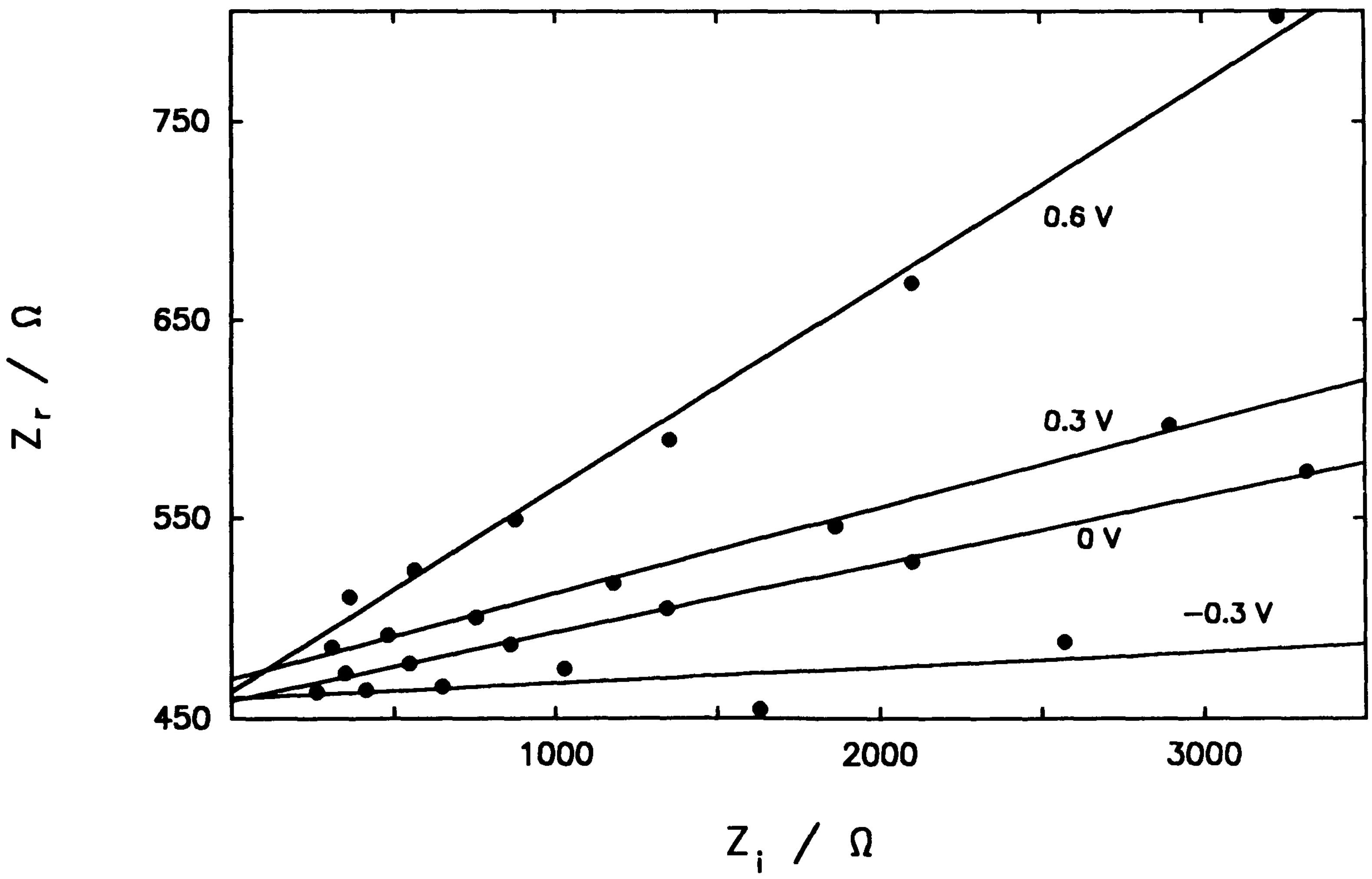

Fig6

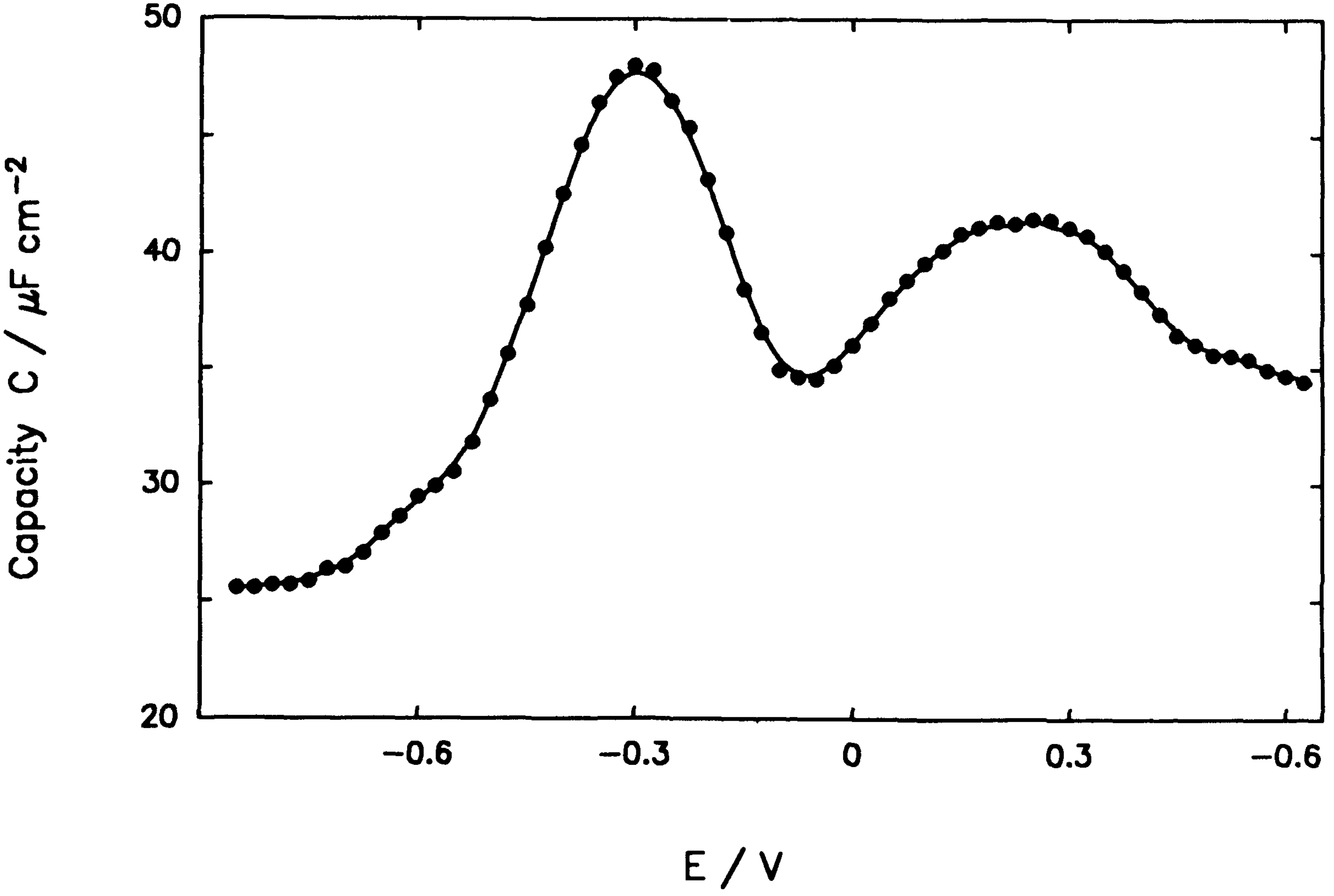

Fig 7

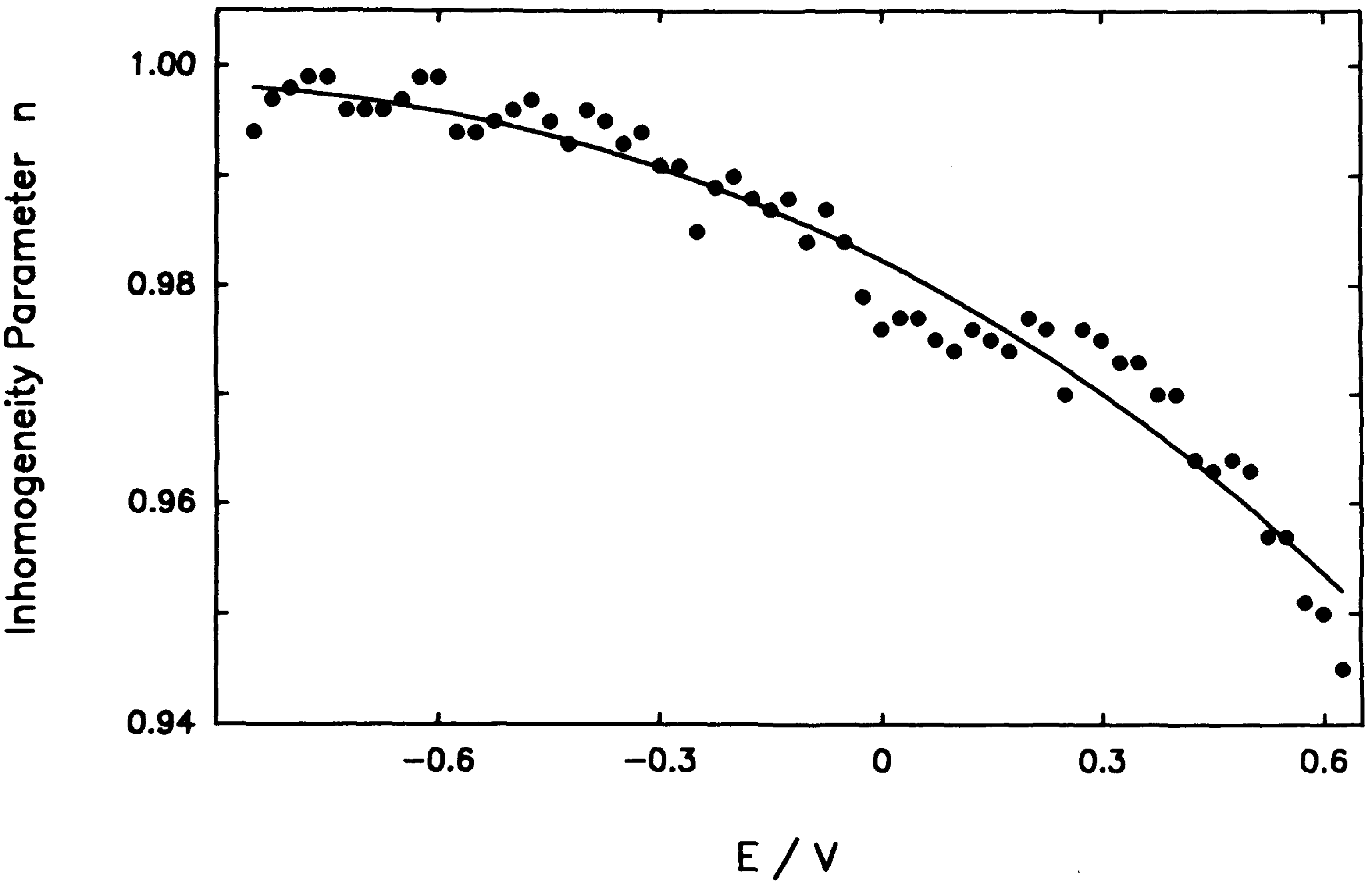

Fig 8

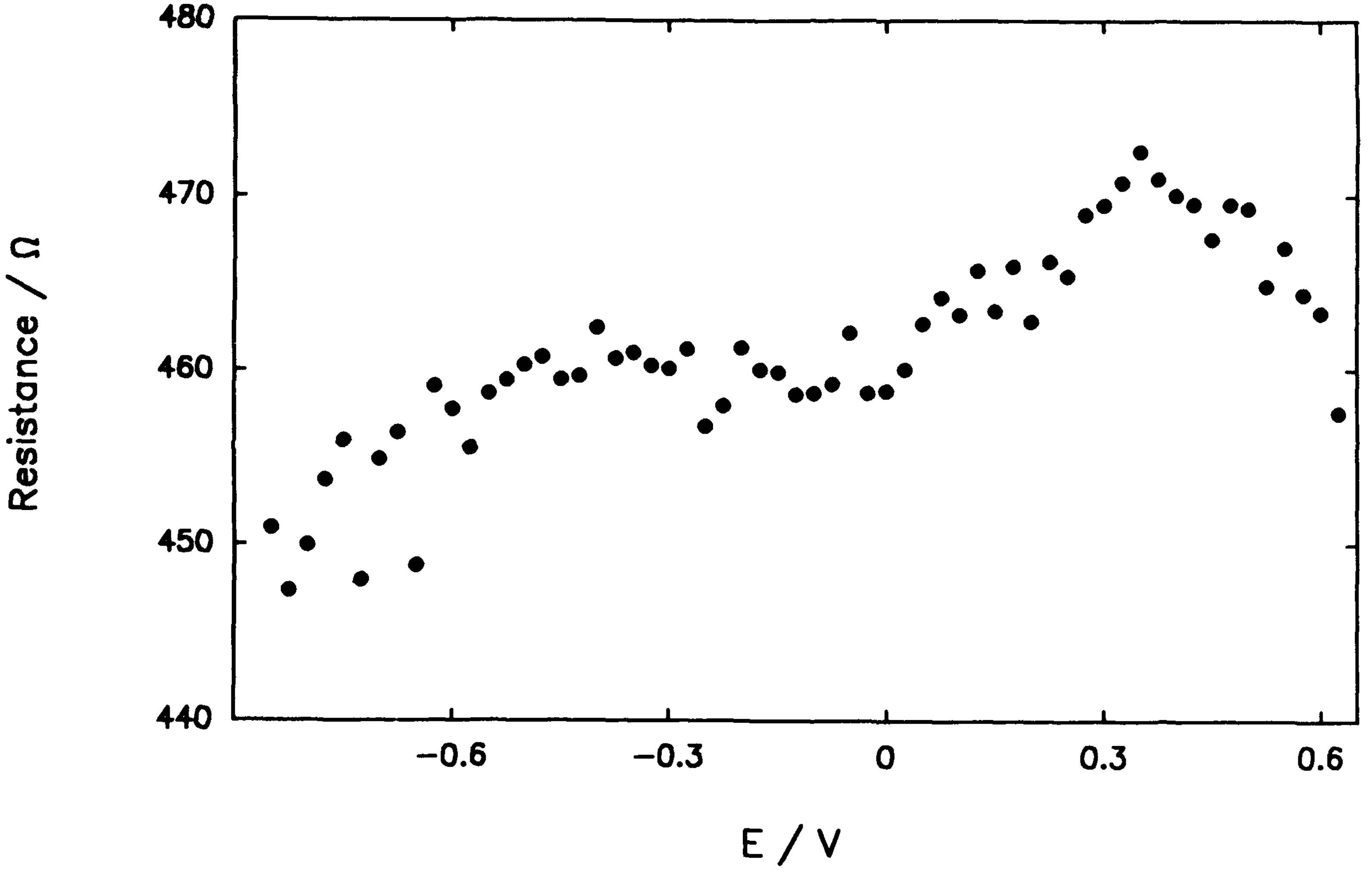

Fig 9